



Universiteit
Leiden
The Netherlands

Future climate impacts of sodium-ion batteries

Zhang, S.; Steubing, B.R.P.; Karlsson Potter, H.; Hansson, P.; Nordberg, Å.

Citation

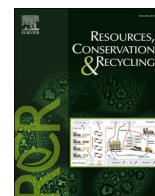
Zhang, S., Steubing, B. R. P., Karlsson Potter, H., Hansson, P., & Nordberg, Å. (2024). Future climate impacts of sodium-ion batteries. *Resources, Conservation And Recycling*, 202. doi:10.1016/j.resconrec.2023.107362

Version: Publisher's Version

License: [Creative Commons CC BY 4.0 license](#)

Downloaded from: <https://hdl.handle.net/1887/3730938>

Note: To cite this publication please use the final published version (if applicable).



Future climate impacts of sodium-ion batteries

Shan Zhang^{a,*}, Bernhard Steubing^b, Hanna Karlsson Potter^a, Per-Anders Hansson^a, Åke Nordberg^a

^a Department of Energy and Technology, Swedish University of Agricultural Sciences, P.O Box 7032 SE-75007, Uppsala, Sweden

^b Institute of Environmental Sciences (CML), Leiden University, 2300, RA Leiden, the Netherlands

ARTICLE INFO

Keywords:

Prospective life cycle assessment
Sodium-ion batteries
Greenhouse gas emissions
Emerging technologies

ABSTRACT

Sodium-ion batteries (SIBs) have emerged as an alternative to lithium-ion batteries (LIBs) due to their promising performance in terms of battery cycle lifetime, safety, operating in wider temperature range, as well as the abundant and low-cost of sodium resources. This study evaluated the climate impacts of three SIBs, and compared to two LIBs under four scenarios with considering potential changes in battery performance and background productions between 2020 and 2050. To ensure a fair comparison, all batteries were modeled in the 21,700 form, and a battery dimensioning model was developed to calculate the required amount of components for each battery. We found that equal to lower GHG emissions result from the use of SIBs compared to LIBs under optimal performance scenarios. From 2020 to 2050, the climate impacts of SIBs decreased by 43–57 %. The relative contribution of the battery manufacturing process decreases from 18–32 % to 2–4 % due to the increasingly share of clean energy in the electricity grid, while the relative contribution of key battery component materials increases over time, especially for cathode active materials. These results emphasize the significance of decarbonizing the electric grid, and suggest that future investment in SIBs is promising from an environmental point of view.

Abbreviation

| | |
|--------|--|
| CMC | Carboxymethyl cellulose |
| DMC | Electrolyte: Dimethyl Carbonate |
| EC | Electrolyte: Ethylene Carbonate |
| EVs | Electric vehicles |
| G | Graphite |
| GHG | Greenhouse gas |
| HC | Hard carbon |
| IAM | Integrated assessment model |
| LCA | Life cycle assessment |
| LCI | Life cycle inventory |
| LFP | Lithium iron phosphate |
| LIB | Lithium ion battery |
| LMO | Lithium manganese oxides |
| NaPBA | Prussian blue analogues $\text{Na}_2\text{FeFe}(\text{CN})_6$ |
| NaPF6 | sodium hexafluorophosphate |
| NMC811 | Lithium nickel manganese cobalt oxide $\text{LiNi}_{0.8}\text{Mn}_{0.1}\text{Co}_{0.1}\text{O}_2$ |
| NMMT | Sodium nickel manganese magnesium titanium oxide, $\text{Na}_{1.1}(\text{Ni}_{0.3}\text{Mn}_{0.5}\text{Mg}_{0.05}\text{Ti}_{0.05})\text{O}_2$ |

| | |
|---------|--|
| NMP | N-methylpyrrolidone |
| NVPF | polyanionic $\text{Na}_3\text{V}_2(\text{PO}_4)_2\text{F}_3$ |
| PE/PP | polyethylene/polypropylene membrane |
| pLCA | prospective life cycle assessment |
| pLCI | prospective life cycle inventory |
| PVDF | Polyvinylidene fluoride |
| SBR | styrene butadiene rubber |
| SIB | Sodium-ion battery |
| VTM ore | vanadium-titanomagnetite ore |

1. Introduction

Batteries play an essential role in the transition to a fossil-free society, as power sources for electric vehicles (EVs), and as storage technologies for intermittent renewable energies. International Energy Agency (IEA) predicted that battery demand for EVs could reach up to 5.6 TWh by 2030 (under Net Zero Emission scenario), which is 16 folds of the demand in 2021 (IEA, 2022). Bogdanov et al. (2019) projected that 48 TWh of battery storage capacity is needed in order to achieve a 100 % renewable electricity system by 2050. Currently, lithium-ion batteries

* Corresponding author.

E-mail address: shan.zhang@slu.se (S. Zhang).

(LIBs) dominate the rechargeable battery market due to their versatility (covering a wide range of applications) and outstanding performance (e.g. high energy density, high power and good lifetime and energy conversion efficiency) (Kim et al., 2019). However, relying solely on LIBs to meet the fast-growing energy storage demand is putting significant pressure on lithium supply chain. This pressure could pose adverse effects on Indigenous people in mining regions (Owen et al., 2023), lead to ecosystem damage (Petavratzi et al., 2022), contribute to a serious lithium supply deficit (Greim et al., 2020), and consequently results in lithium prices increase (Tapia-Ruiz et al., 2021). The short-term availability concerns on lithium supply, in combination with the geographically-constrained reserves and inefficient resource manage-

with two lithium-ion batteries (LIBs). The functional unit (FU) is 1 kWh of energy delivered over the battery's lifetime. This study only considers climate impacts because the integrated assessment model (IAM) used to explore future scenarios focuses on changes in greenhouse gas (GHG) emissions. Given the recent emergence of SIBs in the market, high uncertainty exists in their end-of-life phase, and therefore it was not included in this study. The system boundary includes raw material extraction, transportation, production of precursors, production of battery components, battery manufacturing processes, and use phase by considering the depth of discharge (DoD), lifetime (in cycles) and roundtrip efficiency. The climate impacts associated to battery production is therefore calculated as the following equation:

$$\text{Climate impacts per FU} = \frac{\sum i * IS_i}{\text{specific energy} \times \text{DoD} \times \text{lifetime} \times \text{roundtrip efficiency}} \quad (1)$$

ment in the "lithium triangle" (the lithium reserves abundant region, concluding Bolivia, Chile and Argentina) (Eftekhari, 2019), have raised awareness on the importance of developing alternative battery technologies.

Meanwhile, the increasing amount of research on sodium-ion batteries (SIBs) and the growing numbers of SIB startups show that SIBs are attracting significant attention as a potential alternative to LIBs (Broux et al., 2019; Rudola et al., 2021a). Several companies, such as Faradion in UK (Faradion, 2022), CATL in China (Carla, 2023), Tiamat in France (Tiamat, 2022), Natron from the United States (Natron Energy, 2023), etc. have developed commercial prototypes. This is due to the abundance and low cost of sodium resources, the high safety and long cycle life of SIBs, as well as their excellent performance at cold temperature (Liu et al., 2019; Rudola et al., 2021b). Recent studies also projected that SIBs could cost 10–30 % less than LIBs, indicating them a more affordable energy storage option, especially in developing regions (Abraham, 2020; IEA, 2023; Rudola et al., 2023). Given the fact that sodium ions (Na⁺) has larger atomic radius than lithium ions (Li⁺), the volumetric energy density (Wh/L) of SIBs are intrinsically lower than that of most types of LIBs. Based on predictions and early-stage research results from academia and industry, SIBs could reach comparable specific energy (Wh/kg) to lithium iron phosphate (LFP) batteries (Abraham, 2020; Rudola et al., 2021a). Therefore, SIBs are suitable for applications that do not require high energy density, such as stationary storage and short or medium range electric vehicles (EVs) (Rudola et al., 2023).

Several life cycle assessment (LCA) studies have evaluated the environmental impacts of SIBs (Peters et al., 2016, 2021; Schneider et al., 2019). Additionally, some studies have specifically focused on anode or cathode materials of SIBs (Baumann et al., 2022; Peters et al., 2020; Rey et al., 2022). However, there is a lack of research considering future climate impacts of SIBs. As society undergoes a swift transition towards decarbonization, especially in high energy-intensive sectors, it is expected that the environmental impact of battery cells will be reduced due to the decarbonization of these upstream production processes. Additionally, such transition may alter or uncover environmental hotspots. Therefore, this study aims to perform a prospective life cycle assessment (pLCA) to explore the climate impacts of three promising SIBs produced in 2030, 2040, and 2050, with 2020 as the base year to compare.

2. Materials and method

2.1. Overall approach

Prospective life cycle assessment was conducted to assess future climate impacts of three sodium-ion batteries (SIBs), and to compare

i refers to the amount of battery components and manufacturing energy needed for producing 1 kg of battery, *IS_i* refers to the impact scores (kg CO₂-eq) for producing each unit of battery component and energy. Climate change impacts were computed using IPCC 2013 (100 year time frame) GWP characterization factors. The production of the battery cells was assumed to take place in Europe.

2.2. Life cycle inventory

2.2.1. Battery technologies

Three promising SIBs, with a technology readiness level of 9, were considered in this study based on market and research preference: layered oxide Na_{1.1}(Ni_{0.3}Mn_{0.5}Mg_{0.05}Ti_{0.05})O₂ (NMMT), vanadium-based polyanionic Na₃V₂(PO₄)₂F₃ (NVPF), and Prussian blue analogues Na₂FeFe(CN)₆ (NaPBA). Companies like Faradion Limited, Tiamat, Altris AB, etc., are working on mass-producing the above mentioned battery types (Rudola et al., 2021a; Tapia-Ruiz et al., 2021; Usiskin et al., 2021). To gain a better understanding of the environmental performance of SIBs, two LIBs: LFP and NMC 811 were included for comparison. LFP battery chemistry was selected because SIBs are expected to be used in similar applications as LFP batteries are presently deployed (Abraham, 2020). NMC811 battery chemistry was selected because nickel-rich layered oxide batteries are expected to be dominating the future market to address the urgent demand for energy storage (Kim et al., 2019; Wenjun et al., 2020).

To facilitate a fair comparison, all batteries were designed as the classic 21,700 format, which features a cylindrical shape with a diameter of 21 mm and a height of 70 mm (Fig. 1). Instead of estimating or collecting the percentage of battery components and specific energy values from different literature sources, a battery dimensioning model was established for calculating the amount of each battery material required for studied battery chemistries as well as the corresponding specific energy, which increases the comparability analysis among batteries. The cylindrical cells were manufactured by rolling the battery layers into a cylindrical roll. It was assumed that the thickness of the cylindrical roll (which consists of current collectors, double-side coated electrode, and separators) was uniform at all points, and wound through an Archimedean spiral curve. The amount of each battery component was calculated based on Archimedean spiral curve functions, in combination with thickness of layers or mass loading of electrode active material, physical properties of materials (e.g. density, porosity), and inner volume of battery cell (Waldmann et al., 2020). The above-mentioned parameters use data collected from battery literatures, detailed equations and assumptions can be found in supplementary materials (SM 1 and 2). The cell capacity (mAh), specific energy

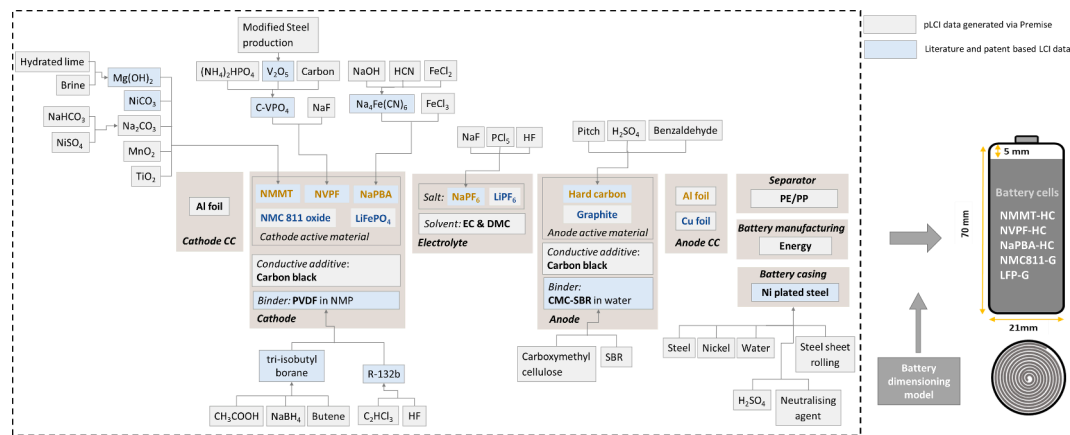


Fig. 1. Materials and energy required for cell production and their data source. Materials and energy within the shadow rectangles are directly used in battery manufacturing, others are upstream materials. Boxes featuring bold yellow words refer to materials only used in SIBs, boxes with bold blue words refer to materials only used in LIBs, boxes with words in bold black refers to materials used in both SIB and LIB. Italic words indicates the names of the battery components. CC refers to current collector; PVDF refers to polyvinylidene fluoride; NMP refers to N-methylpyrrolidone; EC refers to ethylene carbonate; DMC refers to dimethyl carbonate; PE/PP refers to polyethylene/polypropylene membrane.

Table 1

Composition (wt-%) of studied battery cells. HC refers to hard carbon. G refers to graphite. CMC refers to carboxymethyl cellulose. SBR refers to styrene butadiene rubber, super C65 is a high performance conductive carbon black powder.

| | | NMMT//HC | NVPF//HC | NaPBA // HC | NMC811//G | LFP//G |
|-------------------|-------------------------|-----------------------------|-----------------------------|-----------------------------|-----------------------------|-----------------------------|
| Anode | Anode active material | 23.2 % (HC) | 19.2 % (HC) | 18.8 % (HC) | 20.8 % (G) | 17.6 % (G) |
| | Super C65 | 0.8 % | 0.6 % | 0.6 % | 0.4 % | – |
| | CMC-SBR | 1.3 % | 1 % | 1 % | 0.4 % | 0.4 % |
| Cathode | Cathode active material | 31.8 % (NMMT) | 35.5 % (NVPF) | 29.3 % (NaPBA) | 34.0 % (NMC811) | 36.8 % (LFP) |
| | Super C65 | 0.7 % | 0.7 % | 0.6 % | 0.7 % | 0.8 % |
| | PVDF | 0.7 % | 0.7 % | 0.6 % | 0.7 % | 0.8 % |
| Current Collector | Al foil | 8.6 % | 7.2 % | 7.9 % | 13.5 % | 3.3 % |
| | Cu foil | – | – | – | 4.1 % | 11 % |
| Electrolyte | | 16.5 % (NaPF ₆) | 17.6 % (NaPF ₆) | 20.8 % (NaPF ₆) | 13.5 % (LiPF ₆) | 14.3 % (LiPF ₆) |
| Separator | PE/PP | 1.4 % | 1.2 % | 1.3 % | 1.4 % | 1.2 % |
| Cell container | Steel sheet | 15.2 % | 16.1 % | 19 % | 10.5 % | 13.9 % |
| Total weight | | 56.2 g | 53.1 g | 45 g | 64.2 g | 61.4 g |

(Wh/kg), and energy density (Wh/L) of the battery cells was then calculated based on cathode active material capacity (mAh/g), the amount of cathode active material, average voltage of the cell, and the total weight and volume of battery cell (Kevin et al., 2022) (detailed calculation can be found in SM 1 and 2). As a result, NMMT and NaPBA showed comparative specific energies as LIBs, which aligns with the perspective given in Peters et al. (2016). Battery dimensioning model can be found in SM 2. The battery composition results are presented in Table 1.

2.2.2. Data sources

Fig. 1 illustrates the battery materials used in the studied batteries and the life cycle inventory (LCI) data sources. Inventory data for material production and emissions from latest literature and Premise (Sacchi et al., 2022) generated prospective LCI (pLCI) databases was used directly or with modification for battery materials. Further details regarding the generation processes of the pLCI database can be found in Section 2.3.

For cathode active materials, production process and emission data for NMMT and NaPBA were extracted from previous studies (Peters et al., 2016, 2021), while LCI data of NVPF was established using production method described in Bianchini et al. (2014), further details can be read in SM 1. V₂O₅, a precursor in NVPF production process, was modeled as a by-product in primary steel production. The LCI of the steel production process was allocated to the products based on their economic values, a widely adopted allocation method in the ecoinvent database. As a result, 2 wt.% V₂O₅ in the overall products accounted for

36.7 wt.% of the LCI due to its high economic value. The V₂O₅ inventory comprised of 89 % production in China (Chen et al., 2015) and 11 % production in South Africa (Weber et al., 2018), reflecting reorganized market share data from USGS (2022). The production process description and detailed inventory can be found in SM 1 and 2.

As for anode active material, the most commonly used anode material for SIBs: hard carbon, was used. It was modeled using petroleum pitch as precursor due to its high carbon residue and low cost (Xie et al., 2010). The electrolyte is 1 M solution of sodium hexafluorophosphate (NaPF₆) in a mixture solvent of ethylene carbonate (EC) and dimethyl carbonate (DMC) (1:1). NaPF₆ was modeled based on inventory data in Peters et al. (2016). As sodium does not alloy with aluminum at the anode, aluminum foil was used as the current collector for both electrode. It was assumed that the separator of SIBs is identical to that of LIBs, polyethylene/polypropylene (PE/PP) membrane was therefore used in the study. LCI for current collector and separator was from pLCI

Table 2

Energy requirement for battery manufacturing (modified based on Yuan et al. (2017)).

| Battery manufacturing process | Energy consumption |
|---|--------------------------------|
| Electrode mixing and coating, calendaring, notching | 3.8 kWh/ kg electrode |
| Electrodes drying and solvent recycling | 10.6 kWh/ kg recovered solvent |
| Electrolyte filling | 11.2 kWh/kg electrode |
| Dry room operation | 4.1 kWh/kg electrode |

databases. Finally, battery casing is nickel-plated steel sheet, and the production data was from [Chordia et al. \(2021\)](#). When energy consumption data in material production processes not available, it was estimated by methods presented in [Piccinno et al. \(2016\)](#). Detailed inventory generation processes can be found in SM 1 and 2.

Energy needed for battery manufacturing was estimated based on industrial data for manufacturing LMO-graphite battery. Inventory data provided by [Yuan et al. \(2017\)](#) were reorganized and summarized as parameters presented in [Table 2](#). The considered manufacturing processes comprise of electrodes manufacturing (including electrode mixing and coating, calendaring, and notching), electrode drying and solvent recycling; electrolyte filling; and dry room operation. Calculation details can be found in SM 1 and 2. This study assumed electricity to be the only energy source in battery manufacturing processes, an assumption made to align with the reality in giga factories ([Kurland, 2020](#)). The European electricity mixture was used. Note that both battery manufacturing processes and battery composition were assumed to remain the same in the future years.

2.3. Scenario development

To assess the future climate impacts of studied batteries, potential future changes in the upstream systems were considered based on two background scenarios: SSP2-NDC and SSP2-PkBudg500. SSP2 corresponds to the Shared Socioeconomic Pathway narrative 2, representing a continuation of historical development trends in social, economy, and technology aspects ([Riahi et al., 2017](#)). NDCs and PkBudg500 represent two climate targets: national determined contributions and the 1.5 °C Paris Agreement. Following SSP2-NDC and SSP2-PkBudg500 scenarios, the increase of global mean surface temperature can be limited to 2.5 °C and 1.5 °C by 2100 respectively. For simplicity, we refer to these as the "2.5 °C" and "1.5 °C" scenarios in subsequent paragraphs. Another two foreground scenarios captured possible changes in battery performance: "Baseline performance" and "Optimal performance" scenarios. Consequently, this study included four combinations of foreground and background scenarios to explore future changes within the battery system: 2.5 °C - Baseline performance, 1.5 °C - Baseline performance, 2.5 °C - Optimal performance, and 1.5 °C - Optimal performance ([Table 3](#)).

Based on the narrative of these 2.5 °C and 1.5 °C scenarios, integrated assessment model (IAM) REMIND was used to model potential transformation changes in various sectors and regions ([Baumstark et al., 2021](#)), such as future electricity source, fuel generation technologies, improvements in production and process efficiency for energy intensive processes and materials, the implementation of Carbon Capture and Storage (CCS) technology, and shifts in material and energy market share. Next, such transformation changes were used to modify corresponding unit processes in ecoinvent database 3.8 using the Python package Premise ([Sacchi et al., 2022](#)), to generate pLCI databases (Premise: a Python package to integrate IAMs outputs with LCI databases). These pLCI databases were exported in a superstructure format ([Steubing and de Koning, 2021](#)), which was then used to model the total greenhouse gas emission of the battery system in the Activity Browser software ([Steubing et al., 2020](#)).

It is important to note that industry-specific electricity, such as those used by the aluminum, cobalt, and copper industries, were assumed to use the same production processes as current situation. Such assumption is based on the fact that these industries primarily rely on electricity

Table 3
Scenario combinations.

| Scenario names | Background scenarios | Battery performance scenarios |
|-------------------|----------------------|-------------------------------|
| 2.5 °C - Baseline | SSP2-NDC | Baseline performance |
| 1.5 °C - Baseline | SSP2-PkBudg500 | Baseline performance |
| 2.5 °C - Optimal | SSP2-NDC | Optimal performance |
| 1.5 °C - Optimal | SSP2-PkBudg500 | Optimal performance |

generated by internal power plants rather than the general power grid. In addition, fossil fuel power plants such as coal plants have a long lifetime (typically over 50 years) ([Cui et al., 2019](#)). Hence, the private sector would likely economically favor the continued use of existing infrastructure until its designated end of life. Additional details regarding the REMIND model outputs and modifications made in the ecoinvent database can be found in [Sacchi et al. \(2023\)](#).

The Baseline performance scenario refers to the performance that studied batteries could most likely achieve based on current research. Considering the early development of SIBs and the rapid advancements in the field ([Tarascon, 2020](#)), the battery performance may develop faster than expected. Therefore, the best-reported or projected data from battery studies were employed to represent the optimal battery performance. Both battery performance scenarios remain consistent in future years. The technical details of the studied batteries under these two scenarios are presented in [Table 4](#).

The cathode capacity (mAh/g) for each cathode active material in both battery performance scenarios was collected from previous battery studies, and detailed data source can be found in SM 2. Battery lifetime is a parameter characterized by significant uncertainty due to factors such as operation conditions, charging rate, and charging depth ([Han et al., 2019](#)). In this study, we define lifetime as the number of charge–discharge cycles a battery can undergo before reaching 80 % of its initial capacity, with 80 % discharge depth ([Table 4](#)). The baseline performance scenario assumed 4000 cycles for NMMT ([Faradion, 2022](#)) and NMC 811 ([Peters et al., 2021](#)), 5000 cycles for NVPF ([Tiamat, 2022](#)), and 7000 cycles for NaPBA and LFP ([Peters et al., 2021](#)) ([Table 4](#)). The optimal battery lifetime values were derived from the best-reported or projection values ([Peters et al., 2021](#); [Tapia-Ruiz et al., 2021](#); [Xiao et al., 2023](#); [Zhao et al., 2022](#)). Roundtrip efficiency values were based on previous reported value ([Peters et al., 2021](#); [Tapia-Ruiz et al., 2021](#)). Battery voltage and depth discharge remain consistent in both scenario.

3. Results and interpretation

This section is structured as follows: [Section 3.1](#) uncovers the climate impact of batteries in the year 2020, [Section 3.2](#) describes the climate impact of batteries produced in future years (2030, 2040, 2050), and [Section 3.3](#) analyzes the relative contributions of battery materials and energy flows to the overall assessment.

3.1. Climate impacts in 2020

The variation observed in the climate impact results in 2020 was solely due to differences in battery performance scenarios ([Fig. 2](#)). Under the Baseline performance scenarios, the three SIBs demonstrated higher climate impacts compared to LFP (9.8 g CO₂-eq/FU). However, when compared to NMC 811 (18.9 g CO₂-eq/FU), NaPBA (11.8 g CO₂-eq/FU) and NMMT (16.6 g CO₂-eq/FU) displayed better performance in climate impacts. Notably, NVPF had the highest emissions at 22 g CO₂-eq/FU. The results are in line with those from [Peters et al. \(2021\)](#) for NMMT (17 g CO₂-eq/FU), and lower for NaPBA (16.7 g CO₂-eq/FU), due to updated cathode active material capacity data with higher value used in this study.

The disparities in GHG emissions across the studied battery chemistries primarily stem from variations in battery materials used as different material production require varying energy inputs and emit different types of amount of emissions, as well as battery performance-related factors, such as specific energy, cycle life, and roundtrip efficiency. Battery performance factors determines the amount of battery material required to achieve an equivalent FU ([Eq. \(1\)](#)). Consequently, battery chemistries with the optimal combination of these factors exhibit superior climate impact performance. For instance, NaPBA's relatively low climate impacts can be attributed to the low GHG emissions associated with its battery materials, coupled with its extended lifetime, even though its specific energy is the lowest among all

Table 4

Technical details of studied 21,700-size battery cells under baseline and optimal scenario. HC refers to hard carbon, G refers to graphite.

| Scenario | | NMMT/HC | NVPF/HC | NaPBA/ HC | NMC 811 /G | LFP/G | |
|----------------------------------|-----------------------------------|-----------------------------------|---------|-----------|------------|--------|-----|
| Baseline performance | Voltage (V) | 3.2 | 3.4 | 3 | 3.57 | 3.2 | |
| | Cathode specific capacity (mAh/g) | 154 | 120 | 150 | 200 | 157 | |
| | Cell capacity (mAh) | 2748 | 2268 | 1974 | 4361 | 3542 | |
| | Specific energy (Wh/kg) | 157 | 145 | 132 | 243 | 185 | |
| | Volumetric energy density (Wh/L) | 363 | 318 | 244 | 642 | 523 | |
| | Roundtrip efficiency | 94 % | 93 % | 93 % | 91 % | 94 % | |
| | Lifetime (cycles) | 4000 | 5000 | 7000 | 4000 | 7000 | |
| | Discharge Depth | 80 % | 80 % | 80 % | 80 % | 80 % | |
| | Optimal performance | Voltage (V) | 3.2 | 3.4 | 3 | 3.57 | 3.2 |
| | | Cathode specific capacity (mAh/g) | 215 | 138 | 160 | 213 | 165 |
| Cell capacity (mAh) | | 3837 | 2608 | 2106 | 4645 | 3729 | |
| Specific energy (Wh/kg) | | 219 | 232 | 149 | 258 | 194 | |
| Volumetric energy density (Wh/L) | | 506 | 366 | 261 | 684 | 551 | |
| Roundtrip efficiency | | 95 % | 97 % | 97 % | 95 % | 95 % | |
| Lifetime (cycles) | | 8000 | 15,000 | 15,000 | 9000 | 10,500 | |
| Discharge Depth | | 80 % | 80 % | 80 % | 80 % | 80 % | |

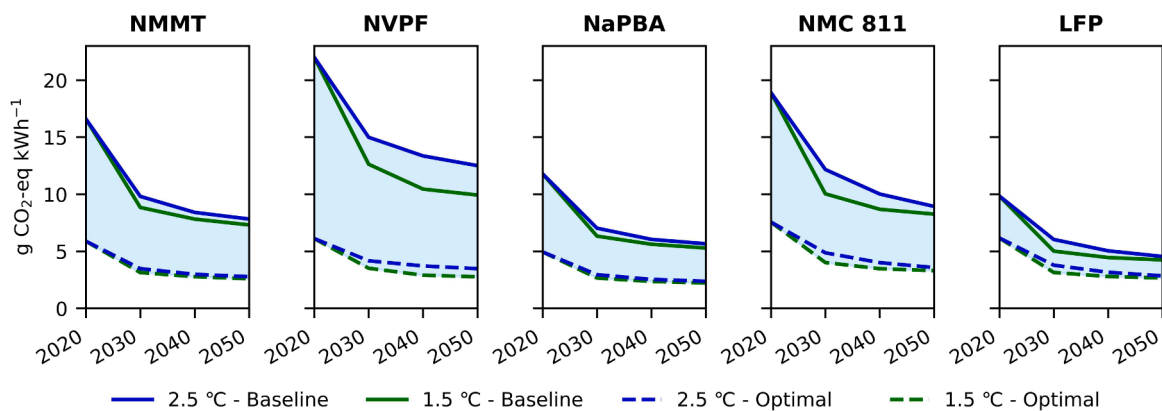


Fig. 2. Climate impacts results of studied batteries at different years, under four scenarios. Results are expressed per kWh of energy delivered along lifetime. The shaded blue area illustrates the disparity in climate impacts resulting from baseline and optimal performance scenarios.

investigated batteries. While the high climate impacts of NVPF can largely be attributed to the high GHG emissions embodied in the precursor material V_2O_5 , as well as the inferior specific energy and cycle life of NVPF.

Applying optimal performance substantially reduced the climate impacts of the studied batteries, resulting in reductions of 65 %, 72 %, 58 %, 60 %, and 37 % for NMMT, NVPF, NaPBA, NMC 811, and LFP, respectively. Consequently, the three SIBs exhibited lower climate impacts than LIBs under Optimal performance scenarios.

3.2. Climate impacts in 2030, 2040, 2050

The total climate impacts for each battery chemistry decreased over time across all four scenarios (Fig. 2). It is important to note that these reductions were primarily driven by the implementation of 1.5 °C and 2.5 °C scenarios, as battery performance was assumed to remain consistent over time. When comparing the production of SIBs in 2050 to that of 2020, the 2.5 °C scenarios exhibited a reduction in climate impacts ranging from 43 % to 54 %, while the 1.5 °C scenarios demonstrated a slightly greater reduction of 55–57 % for studied SIB chemistries. As a result, the GHG emissions for three SIBs (NMMT, NVPF, NaPBA) and two LIBs (NMC 811 and LFP) at year 2050 are: 2.6–7.8 g CO_2 -eq/FU, 2.8–12.5 g CO_2 -eq/FU, 2.2–5.7 g CO_2 -eq/FU, 3.3–8.9 g CO_2 -eq/FU, 2.7–4.5 g CO_2 -eq/FU. This trend is consistent with a recent study by Xu et al. (2022), although they only focused on future climate impacts for LIBs.

These reductions in climate impacts were predominantly attributable to decarbonization efforts within the energy sectors. The REMIND model

projected a remarkable increase in the share of renewable resources (e.g., wind, solar, hydropower) in European electricity generation, rising from 39 % in 2020 to approximately 97–98 % in the 2.5 °C and 1.5 °C scenarios, respectively, by 2050. Consequently, the climate impacts of the European electricity mixture (at medium voltage) dropped from 310 g CO_2 -eq/kWh in 2020 to 13.9–16.3 g CO_2 -eq/kWh in 2050. In addition, the implementation of carbon capture and storage (CCS) technologies in the industrial power and heat generation processes also plays a significant role.

Furthermore, decarbonization strategies in the steel sector, such as improved energy efficiency, the implementation of CCS, and increased recycling and reusing of steel, played a significant role, particularly for NVPF. The GHG emissions of NVPF can be primarily attributed to the production of its precursor material V_2O_5 , which was modeled as a co-product in steel production. Therefore, the 1.5 °C scenarios, with more stringent decarbonization strategies in the steel sector, lead to greater reductions in the climate impacts of NVPF overtime. For example, CCS is implemented in the steel sector under the 1.5 °C scenario but not in the 2.5 °C scenario. This explains the larger discrepancy in climate impact reduction for NVPF between the 2.5 °C and 1.5 °C scenarios compared to other battery chemistries.

3.3. Contribution analysis

Fig. 3 illustrated the contribution analysis under 2.5 °C and 1.5 °C scenarios. Total climate impacts were divided into emissions associated with the production of battery components (including cathode active material, anode active material, current collectors for both electrodes,

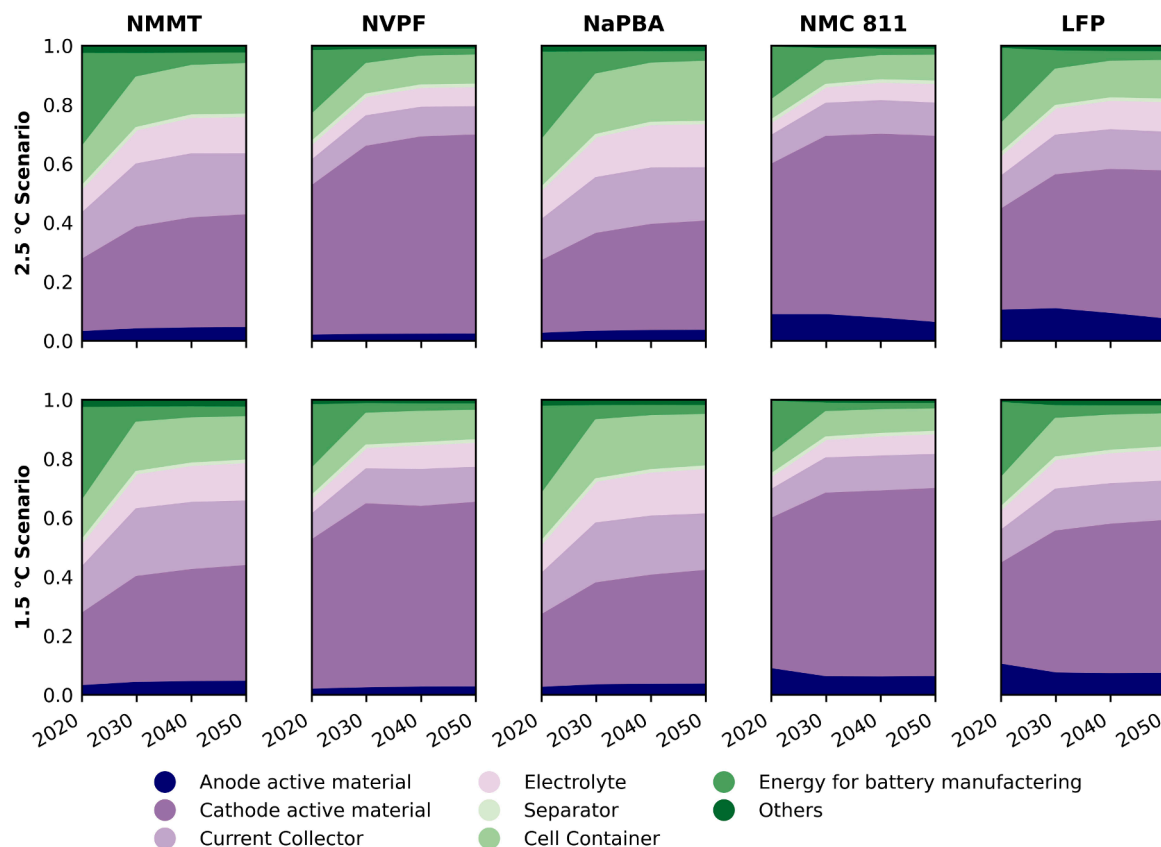


Fig. 3. Relative contributions to overall climate impacts from battery materials and energy use.

electrolyte, and cell container), energy used in battery manufacturing processes, and others (e.g. binders, conductive active material, etc.). Similar contribution results were obtained from both scenarios. It is worth mentioning that battery performance scenarios solely affect the overall climate impacts of batteries and do not impact the relative contributions of material and energy flows.

Cathode active materials were clearly key contributors in all investigated batteries, accounting for a relative contribution of 24–39 % for NMMT, 51–67 % for NVPF, 25–39 % for NaPBA, 51–64 % for NMC 811, and 34–52 % for LFP, regardless of the production year and applied scenarios. The relative contribution of cathode for NMMT and NaPBA is lower than that of LIBs, while the relative contribution of NVPF is higher than that of LIBs. The significant contribution of cathode active materials stemmed from mineral mining and processing steps (e.g., cobalt, nickel, vanadium oxide), high-emission production processes such as hydrogen cyanide production, and the substantial proportion of cathode active material in the battery cell by weight (Table 1). The relatively high contribution from cathode active material of NVPF is primarily associated with the production of precursor material V_2O_5 . As described earlier, V_2O_5 is modeled as a by-product of primary steel production, a highly energy-intensive process. The economic allocation choice results in V_2O_5 with 2 wt.% of the overall products accounted for 36.7 % of the emissions due to its high economic value. The relatively high contribution from cathode active material in NMC 811 can be attributed to the production of precursor materials: cobalt sulfate and nickel sulfate, both related to cobalt production. Nickel sulfate was modeled as a co-product in the cobalt production processes. Nickel sulfate was also a raw material used in the production of cathode active material for NMMT, but 66 % less nickel sulfate is consumed in producing per kg of cathode active material in NMMT compared to that used in producing per kg of cathode active material in NMC 811.

Energy consumption during the battery manufacturing process emerged as another notable contributor to total emissions for the three

studied SIBs at 2020, accounting for 18–32 % of total emissions. This substantial energy consumption in battery manufacturing processes can be primarily attributed to operations such as drying and solvent recovery (NMP) of the binder, dry room operation, and electrolyte filling. The finding is consistent with previous studies highlighting battery manufacturing as a significant source of GHG emissions (Peters et al., 2021; Schneider et al., 2019).

Additionally, the production of current collector (9–16 %), cell container (7–16 %), and electrolyte (5–10 %) are other important contributors to total GHG emissions of studied SIB chemistries at 2020. These emissions arise from manufacturing processes involving producing aluminum foil (current collector), and steel (cell container material). On the other hand, the production of the anode active material (1–3 %), namely hard carbon, made a minor contribution to the overall climate impacts in SIBs in 2020, despite accounting for 19–23 wt-% of the battery cell. Similar trends were also observed in Peters et al. (2021). In contrast, the anode active material in LIBs (graphite) contributed 8–10 % to total emissions in 2020, primarily due to the higher manufacturing temperature required for graphite than for hard carbon production.

From 2020 to 2050, significant contribution reductions from the battery manufacturing stage can be observed, which is due to the decarbonization in European electricity mixture. The decreased GHG emissions from the battery manufacturing process contributed to up to 66 % of the total reduction in climate impacts of investigated batteries. Consequently, the GHG emissions from the battery manufacturing process account for only 2–4 % of the total impacts in both scenarios by 2050. In contrast, the relative contribution from other material flows are likely to increase over time.

3.4. Sensitivity analysis

Notably, the choice of allocation methods can significantly influence the climate impacts of V_2O_5 (He et al., 2020), thus affecting the total

GHG emissions of the NVPF battery. He et al. (2020) highlighted the influence of allocation method on the environmental impacts of V_2O_5 , when modeling it as a by-product of steel production. In this sensitivity analysis, we changed the allocation method used in production of V_2O_5 and crude steel from economic allocation to mass-based allocation. The sensitivity analysis results reveals a significant reduction of 40 % in the total climate impacts of NVPF battery, resulting in a similar environmental impacts as NaPBA (11.7 CO_2 -eq/FU) in 2020.

4. Discussion

This study for the first time assessed the future climate impacts of SIBs while considering potential changes in both the foreground and upstream aspects of the battery system. Lai et al. (2023) conducted an LCA on various sodium battery technologies using future Chinese electricity mixtures in the battery manufacturing processes, without considering potential future changes in the background system. This likely explains the significant disparity in future GHG emission results, which were up to five times higher than our findings when converted to the same FU.

The results underscore the critical importance of optimizing battery performance, a measure that can mitigate more climate impacts per FU than the decarbonization of energy-intensive sectors within the upstream system. This aligns with prior research emphasizing the significance of specific energy and battery lifetime in environmental impacts (Peters et al., 2017; Schneider et al., 2019). This insight could guide future research directions aimed at fostering the sustainable development of batteries. For instance, the scenario results suggested that enhancing the specific capacity (mAh/g) of the electrode active material could reduce the climate impacts of the cell. Additionally, modifying cell dimensions can also affect the climate impacts by influencing the specific energy of the cell.

Furthermore, the results highlight the SIBs' potential to either outperform or at least match LIBs in terms of climate impact, with optimization. This speaks in favor of supporting the further development of SIBs. Despite this potential, EU funding for SIB research has been minimal, accounting for only 2.5 % of public funding in battery research from 2014 to 2021 (Bielewski et al., 2022). SIBs offer a cost-effective alternative for stationary and vehicle applications, especially in developing regions and sectors prioritizing affordability, such as buses and trucks. Notably, over 50 % of truck consumers rely on leasing or loans for their purchases (IEA, 2023). Therefore, increased investment in SIB research holds the key to increasing its market penetration significantly and enhancing its climate impact performance.

Increasing the share of renewable energy in the power grid and steel industries and implementing CCS are also important for reducing GHG emissions in battery production. Achieving this requires concerted efforts not only from battery manufacturers but also from industries involved in the entire battery production chain, including electricity, heat and power, steel, and others. Future battery or battery component factories could consider locating near clean energy sources like hydro-power, wind, or solar energy to further mitigate emissions.

An advantage of SIBs is their reduced reliance on critical materials such as cobalt and lithium, which were not assessed in this study. We conducted rough calculation based on scenarios presented in Xu et al. (2020) and the Electric Vehicles (EVs) development trend outlined in IEA (2023). Assuming 100 % market penetration of EVs by 2050 and a 60 % market share of LFP chemistry in EVs between 2030 and 2050, if SIBs could replace LFP entirely, the lithium demand could be reduced as much as 16.4 Mt by 2050. This equals to more than 50 % of current low-cost lithium resources (Greim et al., 2020). However, it is important to note that substituting LIBs with SIBs may increase demand for other materials like nickel, manganese, and vanadium.

There are other perspectives that have not been considered in this study. First, our focus was solely on climate impacts. This is because current scenarios and IAMs have detailed representations of narratives

and sectors relevant to climate impacts, but do not have a specific focus on other environmental impact categories (Steubing et al., 2023). Future research should extend its scope to consider other environmental impact categories for a more comprehensive understanding and to avoid potential environmental burden shifting. To achieve this, a more comprehensive pLCI database need to be developed by including the future changes in sectors and environmental interventions related to other impact categories in IAMs (Steubing et al., 2023). Second, this study assessed battery chemistries at the cell level. In various applications, batteries are often used in modules and packs, with additional components like battery management systems and packages. According to Peters and Weil (2018), the average climate impacts for these additional battery components are approximately 2.2 $kgCO_2$ -eq/kg battery. This suggests that the climate impacts of batteries at the module /pack are likely to favor battery chemistries with an optimal combination of performance (e.g. higher specific energy, longer cycle life). This is due to the correlation between higher performance and the need for fewer batteries, thereby resulting in lower greenhouse gas emissions. The environmental performance at module/pack level also depends on the specific design considerations, which could be explored in the future research. Third, we did not consider advancements in battery manufacturing method, which could lead to more efficient processes. However, our results indicate a relatively minor contribution from battery manufacturing processes when clean electricity is used. Moreover, end-of-life (EoL) stage of SIBs was not considered, as the primary focus was on battery production. EoL options, such as repurposing batteries for other applications or recycling raw materials, could mitigate environmental impacts over the battery's lifetime. While repurposing may not affect the relative environmental performance order among studied batteries, recycling battery raw materials may favor battery chemistries using minerals with high GHG emissions, such as NVPF and NMC 811. However, the economic viability of recycling SIBs remains uncertain due to their lower economic value compared to LIBs. What's more, this study used fossil-based precursors for hard carbon (anode active material) in the model due to its low cost and high carbon residue. While extensive research has explored the use of biomass as a precursor to produce hard carbon, previous studies have highlighted that SIBs with biomass-based hard carbon anode generally show higher climate impacts compared to fossil-based alternatives (Peters et al., 2019). Among various organic precursors, organic waste like apple pomace demonstrates favorable climate impact performance (Peters et al., 2019). However, addressing the challenge of ensuring consistency in organic flow and content is crucial to secure a robust supply chain. Last but not least, the rapid development of other promising battery technologies, like all-solid-state sodium ion batteries, requires future studies to assess their environmental performance, which falls outside the scope of this study.

5. Conclusion

Based on the functional unit of 1 kWh of energy delivered over lifetime, the results show that sodium-ion batteries (SIBs) have the potential to perform equal or better in climate impacts than lithium-ion batteries. Achieving this potential requires efforts and increased investment in SIBs research and development by battery researchers. The climate impacts of SIBs exhibited a reduction of 43–57 % by 2050 compared to their 2020 levels. This reduction is primarily attributed to the increasing penetration of renewable energy sources in the grid electricity mix and substantial decarbonization efforts undertaken within the steel sector. The relative contribution of battery manufacturing processes to the total emission decrease significantly over time, while the relative contribution of cathode active material increase over time. Existing battery industries can prioritize the use of clean energy sources for manufacturing batteries to mitigate their climate impacts. Future battery facilities may consider strategic locations close to regions where clean energy is abundantly produced.

Moreover, sensitivity analyses underscore the impact of allocation methods used in precursor material of the NVPF's cathode active material on results.

CRedit authorship contribution statement

Shan Zhang: Conceptualization, Methodology, Software, Formal analysis, Investigation, Writing – original draft, Writing – review & editing, Visualization. **Bernhard Steubing:** Methodology, Writing – review & editing. **Hanna Karlsson Potter:** Supervision, Writing – review & editing. **Per-Anders Hansson:** Supervision, Funding acquisition. **Åke Nordberg:** Supervision, Writing – review & editing.

Declaration of Competing Interest

The authors declare that they have no known competing financial interests or personal relationships that could have appeared to influence the work reported in this paper.

Data availability

Data will be made available on request.

Acknowledgements

This work was supported by the Department of Energy and Technology, Swedish University of Agricultural Sciences and Mistra Food Futures research programme (Grant ID: DIA 2018/24). The authors would like to thank Romain Sacchi for his great support in understanding Premise and Ioan-Robert Istrate for helping with the result visualization.

Supplementary materials

Supplementary material associated with this article can be found, in the online version, at [doi:10.1016/j.resconrec.2023.107362](https://doi.org/10.1016/j.resconrec.2023.107362).

References

- Abraham, K.M., 2020. How comparable are sodium-ion batteries to lithium-ion counterparts? *Acs Energy Lett.* 5 (11), 3544–3547. <https://doi.org/10.1021/acseenergylett.0c02181>.
- Baumann, M., Häringer, M., Schmidt, M., Schneider, L., Peters, J.F., Bauer, W., Weil, M., 2022. Prospective sustainability screening of sodium-ion battery cathode materials. *Adv. Energy Mater.*, 2202636.
- Baumstark, L., Bauer, N., Benke, F., Bertram, C., Bi, S., Gong, C.C., Luderer, G., 2021. REMIND2.1: transformation and innovation dynamics of the energy-economic system within climate and sustainability limits. *Geosci. Model Dev.* 14 (10), 6571–6603. <https://doi.org/10.5194/gmd-14-6571-2021>.
- Bianchini, M., Brisset, N., Fauth, F., Weill, F., Elkaim, E., Suard, E., Croguennec, L., 2014. Na3V2(PO4)2F3 revisited: a high-resolution diffraction study. *Chem. Mater.* 26 (14), 4238–4247. <https://doi.org/10.1021/cm501644g>.
- Bielewski, M., Pfrang, A., Bobba, S., Kronberga, A., Georgakaki, A., Letout, S., Grabowska, M., 2022. Clean Energy Technology Observatory: Batteries for Energy Storage in the European Union - 2022 Status Report on Technology Development, Trends, Value Chains and Markets. Retrieved from Luxembourg.
- Bogdanov, D., Farfan, J., Sadovskaia, K., Aghahosseini, A., Child, M., Gulagi, A., Breyer, C., 2019. Radical transformation pathway towards sustainable electricity via evolutionary steps. *Nat. Commun.* 10. <https://doi.org/10.1038/s41467-019-08855-1>. ARTN 1077.
- Broux, T., Fauth, F., Hall, N., Chatillon, Y., Bianchini, M., Bamine, T., Reynier, Y., 2019. High rate performance for carbon-coated Na3V2(PO4)2F3 in Na-ion batteries. *Small Methods* 3 (4), 1800215.
- Carla, W. (2023). CATL and BYD to use sodium-ion batteries in EVs this year. Retrieved from <https://www.electrive.com/2023/04/21/catl-and-byd-to-use-sodium-ion-batteries-in-evs-this-year/>.
- Chen, S.Y., Fu, X.J., Chu, M.S., Liu, Z.G., Tang, J., 2015. Life cycle assessment of the comprehensive utilisation of vanadium titanomagnetite. *J. Clean. Prod.* 101, 122–128. <https://doi.org/10.1016/j.jclepro.2015.03.076>.
- Chordia, M., Nordelöf, A., Ellingsen, L.A.-W., 2021. Environmental life cycle implications of upscaling lithium-ion battery production. *Int. J. Life Cycle Assess.* 26, 2024–2039.
- Cui, R.Y., Hultman, N., Edwards, M.R., He, L., Sen, A., Surana, K., Shearer, C., 2019. Quantifying operational lifetimes for coal power plants under the Paris goals. *Nat. Commun.* 10, 4759. <https://doi.org/10.1038/s41467-019-12618-3>.
- Eftekhari, A., 2019. Lithium batteries for electric vehicles: from economy to research strategy. *ACS Sustain. Chem. Eng.* 7 (6), 5602–5613. <https://doi.org/10.1021/acscuschemeng.8b01494>.
- Faradion. (2022). Technology benefits: strong performance. Retrieved from <https://faradion.co.uk/technology-benefits/strong-performance/>.
- Greim, P., Solomon, A., Breyer, C., 2020. Assessment of lithium criticality in the global energy transition and addressing policy gaps in transportation. *Nat. Commun.* 11 (1), 1–11.
- Han, X.B., Lu, L.G., Zheng, Y.J., Feng, X.N., Li, Z., Li, J.Q., Ouyang, M.G., 2019. A review on the key issues of the lithium ion battery degradation among the whole life cycle. *Etransportation* 1, 100005. <https://doi.org/10.1016/j.etrans.2019.100005>. ARTN.
- He, H.Y., Tian, S., Tarroja, B., Oguseitan, O.A., Samuelsen, S., Schoenung, J.M., 2020. Flow battery production: materials selection and environmental impact. *J. Clean. Prod.* 269, 121740. <https://doi.org/10.1016/j.jclepro.2020.121740>. ARTN.
- IEA, 2022. *World Energy Outlook*. International Energy Agency: IEA, Paris.
- IEA, 2023. *Global EV Outlook 2023*. Retrieved from Paris: <https://www.iea.org/report/global-ev-outlook-2023>.
- Kevin, W., .K., Joseph, J., .K., Paul, A., .N., Shabbir, A., 2022. Battery Performance and Cost Modeling For Electric-Drive Vehicles. Retrieved from.
- Kim, T., Song, W.T., Son, D.Y., Ono, L.K., Qi, Y.B., 2019. Lithium-ion batteries: outlook on present, future, and hybridized technologies. *J. Mater. Chem. A* 7 (7), 2942–2964. <https://doi.org/10.1039/c8ta10513h>.
- Kurland, S.D., 2020. Energy use for GWh-scale lithium-ion battery production. *Environ. Res. Commun.* 2 (1), 012001. <https://doi.org/10.1088/2515-7620/ab5e1e>. ARTN.
- Lai, X., Chen, J., Chen, Q., Han, X., Lu, L., Dai, H., Zheng, Y., 2023. Comprehensive assessment of carbon emissions and environmental impacts of sodium-ion batteries and lithium-ion batteries at the manufacturing stage. *J. Clean. Prod.*, 138674.
- Liu, T.F., Zhang, Y.P., Jiang, Z.G., Zeng, X.Q., Ji, J.P., Li, Z.H., Liang, C.D., 2019. Exploring competitive features of stationary sodium ion batteries for electrochemical energy storage. *Energy Environ. Sci.* 12 (5), 1512–1533. <https://doi.org/10.1039/c8ee03727b>.
- Natron Energy, 2023. *Natron Energy*.
- Owen, J.R., Kemp, D., Lechner, A.M., Harris, J., Zhang, R.L., Lèbre, É., 2023. Energy transition minerals and their intersection with land-connected peoples. *Nat. Sustain.* 6 (2), 203. <https://doi.org/10.1038/s41893-022-00994-6>. +.
- Petavratzi, E., Sanchez-Lopez, D., Hughes, A., Stacey, J., Ford, J., Butcher, A., 2022. The impacts of environmental, social and governance (ESG) issues in achieving sustainable lithium supply in the lithium triangle. *Miner. Econ.* 35 (3–4), 673–699. <https://doi.org/10.1007/s13563-022-00332-4>.
- Peters, J., Buchholz, D., Passerini, S., Weil, M., 2016. Life cycle assessment of sodium-ion batteries. *Energy Environ. Sci.* 9 (5), 1744–1751. <https://doi.org/10.1039/c6ee00640j>.
- Peters, J.F., Abdelbaky, M., Baumann, M., Weil, M., 2019. A review of hard carbon anode materials for sodium-ion batteries and their environmental assessment. *Mater. Tech.* 107 (5), 503.
- Peters, J.F., Abdelbaky, M., Baumann, M., Weil, M., 2020. A review of hard carbon anode materials for sodium-ion batteries and their environmental assessment. *Mater. Tech.* 107 (5), 503. <https://doi.org/10.1051/mattech/2019029>. ARTN.
- Peters, J.F., Baumann, M., Binder, J.R., Weil, M., 2021. On the environmental competitiveness of sodium-ion batteries under a full life cycle perspective - a cell-chemistry specific modelling approach. *Sustain. Energy Fuels* 5 (24), 6414–6429. <https://doi.org/10.1039/d1se01292d>.
- Peters, J.F., Baumann, M., Zimmermann, B., Braun, J., Weil, M., 2017. The environmental impact of Li-ion batteries and the role of key parameters - a review. *Renew. Sustain. Energy Rev.* 67, 491–506. <https://doi.org/10.1016/j.rser.2016.08.039>.
- Peters, J.F., Weil, M., 2018. Providing a common base for life cycle assessments of Li-ion batteries. *J. Clean. Prod.* 171, 704–713. <https://doi.org/10.1016/j.jclepro.2017.10.016>.
- Piccinno, F., Hischer, R., Seeger, S., Som, C., 2016. From laboratory to industrial scale: a scale-up framework for chemical processes in life cycle assessment studies. *J. Clean. Prod.* 135, 1085–1097. <https://doi.org/10.1016/j.jclepro.2016.06.164>.
- Rey, I., Iturrondobeitia, M., Akizu-Gardoki, O., Minguez, R., Lizundia, E., 2022. Environmental impact assessment of Na3V2(PO4)3 cathode production for sodium-ion batteries. *Adv. Energy Sustain. Res.* 3 (8), 2200049. <https://doi.org/10.1002/aesr.202200049>. ARTN.
- Riahi, K., van Vuuren, D.P., Kriegler, E., Edmonds, J., O'Neill, B.C., Fujimori, S., Tavoni, M., 2017. The shared socioeconomic pathways and their energy, land use, and greenhouse gas emissions implications: an overview. *Glob. Environ. Change-Human Policy Dimens.* 42, 153–168. <https://doi.org/10.1016/j.gloenvcha.2016.05.009>.
- Rudola, A., Rennie, A.J.R., Heap, R., Meysami, S.S., Lowbridge, A., Mazzali, F., Barker, J., 2021a. Commercialisation of high energy density sodium-ion batteries: faradion's journey and outlook. *J. Mater. Chem. A* 9 (13), 8279–8302. <https://doi.org/10.1039/d1ta00376c>.
- Rudola, A., Sayers, R., Wright, C.J., Barker, J., 2023. Opportunities for moderate-range electric vehicles using sustainable sodium-ion batteries. *Nat. Energy*. <https://doi.org/10.1038/s41560-023-01215-w>.
- Rudola, A., Wright, C.J., Barker, J., 2021b. Reviewing the safe shipping of lithium-ion and sodium-ion cells: a materials chemistry perspective. *Energy Mater. Adv.* 2021, 9798460. <https://doi.org/10.34133/2021/9798460>. Artin.
- Sacchi, R., Terlouw, T., Siala, K., Dirmaichner, A., Bauer, C., Cox, B., Luderer, G., 2022. PRospective EnvironMental Impact asSEment (premise): a streamlined approach to

- producing databases for prospective life cycle assessment using integrated assessment models. *Renew. Sustain. Energy Rev.* 160, 112311 <https://doi.org/10.1016/j.rser.2022.112311>. ARTN.
- Sacchi, R., Dirnaichner, A., & Mutel, C. (2023). *Premise: Release 1.5.0-alpha*. Retrieved from https://premise.readthedocs.io/_/downloads/en/latest/pdf/.
- Schneider, S.F., Bauer, C., Novak, P., Berg, E.J., 2019. A modeling framework to assess specific energy, costs and environmental impacts of Li-ion and Na-ion batteries. *Sustain. Energy Fuels* 3 (11), 3061–3070. <https://doi.org/10.1039/c9se00427k>.
- Steubing, B., Beltran, A.M., Sacchi, R., 2023. Conditions for the broad application of prospective life cycle inventory databases. *Int. J. Life Cycle Assess.* 28 (9), 1092–1103. <https://doi.org/10.1007/s11367-023-02192-8>.
- Steubing, B., de Koning, D., 2021. Making the use of scenarios in LCA easier: the superstructure approach. *Int. J. Life Cycle Assess.* 26 (11), 2248–2262. <https://doi.org/10.1007/s11367-021-01974-2>.
- Steubing, B., de Koning, D., Haas, A., Mutel, C.L., 2020. The activity browser - an open source LCA software building on top of the brightway framework. *Softw. Impacts* 3, 100012. <https://doi.org/10.1016/j.simpa.2019.100012>. ARTN.
- Tapia-Ruiz, N., Armstrong, A.R., Alptekin, H., Amores, M.A., Au, H.T., Barker, J., Younesi, R., 2021. 2021 roadmap for sodium-ion batteries. *J. Phys.-Energy* 3 (3), 031503. <https://doi.org/10.1088/2515-7655/ac01ef>. ARTN.
- Tarascon, J.-M., 2020. Na-ion versus Li-ion batteries: complementarity rather than competitiveness. *Joule* 4 (8), 1616–1620.
- Tiamat. (2022). Retrieved from <http://www.tiamat-energy.com/>.
- USGS, 2022. *Mineral Commodity Summaries Vanadium*. Reston, VA. Retrieved from.
- Usiskin, R., Lu, Y.X., Popovic, J., Law, M., Balaya, P., Hu, Y.S., Maier, J., 2021. Fundamentals, status and promise of sodium-based batteries. *Nat. Rev. Mater.* 6 (11), 1020–1035. <https://doi.org/10.1038/s41578-021-00324-w>.
- Waldmann, T., Scurtu, R.G., Richter, K., Wohlfahrt-Mehrens, M., 2020. 18650 vs. 21700 Li-ion cells - a direct comparison of electrochemical, thermal, and geometrical properties. *J. Power Sources* 472, 228614. <https://doi.org/10.1016/j.jpowsour.2020.228614>. ARTN.
- Weber, S., Peters, J.F., Baumann, M., Weil, M., 2018. Life cycle assessment of a vanadium redox flow battery. *Environ. Sci. Technol.* 52 (18), 10864–10873. <https://doi.org/10.1021/acs.est.8b02073>.
- Wenjun, L., Hangyu, X., Qi, Y., Jiuming, L., Zhenyu, Z., Shengbin, W., Zhen, Z., 2020. Development of strategies for high-energy-density lithium batteries. *Energy Storage Sci. Technol.* 9 (2), 448.
- Xiao, L.F., Ji, F.J., Zhang, J.X., Chen, X.M., Fang, Y.J., 2023. Doping regulation in polyanionic compounds for advanced sodium-ion batteries. *Small* 19 (1). <https://doi.org/10.1002/sml.202205732>.
- Xie, Q.S., Qiao, Y.M., Du, X., & Wu, M.C. (2010). China Patent No. CN201010566309A.
- Xu, C., Dai, Q., Gaines, L., Hu, M., Tukker, A., Steubing, B., 2020. Future material demand for automotive lithium-based batteries. *Commun. Mater.* 1 (1), 1–10.
- Xu, C., Steubing, B., Hu, M., Harpprecht, C., van der Meide, M., Tukker, A., 2022. Future greenhouse gas emissions of automotive lithium-ion battery cell production. *Resour., Conserv. Recycl.* 187, 106606.
- Yuan, C., Deng, Y.L., Li, T.H., Yang, F., 2017. Manufacturing energy analysis of lithium ion battery pack for electric vehicles. *Cirp Ann.-Manuf. Technol.* 66 (1), 53–56. <https://doi.org/10.1016/j.cirp.2017.04.109>.
- Zhao, L., Zhang, T., Li, W., Li, T., Zhang, L., Zhang, X., Wang, Z., 2022. Engineering of sodium-ion batteries: opportunities and challenges. *Engineering*.